OXFORD

ORIGINAL ARTICLE

RAGE mediates Aβ accumulation in a mouse model of Alzheimer's disease via modulation of β- and γ-secretase activity

Fang Fang[1], Qing Yu[1], Ottavio Arancio[2], Doris Chen[1], Smruti S. Gore[1], Shirley ShiDu Yan[1,*] and Shi Fang Yan[1,*]

[1]Department of Pharmacology and Toxicology, and Higuchi Bioscience Center, School of Pharmacy, University of Kansas, Lawrence, KS 66047, USA and [2]Department of Pathology and Taub Institute for Research on Aging and Alzheimer's Disease, Physicians & Surgeons College of Columbia University, New York, NY 10032, USA

*To whom correspondence should be addressed at: Department of Pharmacology and Toxicology, and Higuchi Bioscience Center, School of Pharmacy, University of Kansas, 2099 Constant Ave., Lawrence, KS 66047, USA. Tel: +1 7858641987; Email: sfangyan@ku.edu (S.F.Y.); Tel: +1 7858643637; Email: shidu@ku.edu (S.S.Y.)

Abstract

Receptor for Advanced Glycation End products (RAGE) has been implicated in amyloid β-peptide (Aβ)-induced perturbation relevant to the pathogenesis of Alzheimer's disease (AD). However, whether and how RAGE regulates Aβ metabolism remains largely unknown. Aβ formation arises from aberrant cleavage of amyloid pre-cursor protein (APP) by β- and γ-secretase. To investigate whether RAGE modulates β- and γ-secretase activity potentiating Aβ formation, we generated mAPP mice with genetic deletion of RAGE (mAPP/RO). These mice displayed reduced cerebral amyloid pathology, inhibited aberrant APP-Aβ metabolism by reducing β- and γ-secretases activity, and attenuated impairment of learning and memory compared with mAPP mice. Similarly, RAGE signal transduction deficient mAPP mice (mAPP/DN-RAGE) exhibited the reduction in Aβ40 and Aβ42 production and decreased β-and γ-secretase activity compared with mAPP mice. Furthermore, RAGE-deficient mAPP brain revealed suppression of activation of p38 MAP kinase and glycogen synthase kinase 3β (GSK3β). Finally, RAGE siRNA-mediated gene silencing or DN-RAGE-mediated signaling deficiency in the enriched human APP neuronal cells demonstrated suppression of activation of GSK3β, accompanied with reduction in Aβ levels and decrease in β- and γ-secretases activity. Our findings highlight that RAGE-dependent signaling pathway regulates β- and γ-secretase cleavage of APP to generate Aβ, at least in part through activation of GSK3β and p38 MAP kinase. RAGE is a potential therapeutic target to limit aberrant APP-Aβ metabolism in halting progression of AD.

Introduction

Cerebral amyloid plaques are characteristic lesions found in Alzheimer's disease (AD) and are composed of amyloid-β (Aβ) peptide, including Aβ1–40 and Aβ1–42, which are the endoproteolytic derivatives from amyloid pre-cursor protein (APP) (1). Aβ formation involves sequential cleavage of APP by proteolytic reactions of β- and γ-secretase (2–5). β-Secretase mediates APP cleavage to form the amino (N)-terminus of Aβ and yield the membrane bound C-terminal fragment CTFβ (3). Next, γ-secretase cleaves CTFβ to release Aβ peptide and APP intracellular C-terminal domain (AICD), a 6-KD peptide also called CTFγ (4). Excessive Aβ production, aggregation, and deposition arise from aberrant APP metabolism that is thought to be an underlying

cause of neurodegenerative outcomes in AD. Given that the accumulation of aggregated Aβ is associated with AD progression and both β- and γ-secretase are pre-requisite for APP processing to generate Aβ, much work have focused on choosing either or both of these proteases as prime drug targets aim to lower Aβ levels in halting AD progression. Several drugs exerted modifying or controlling influences on the activity of these secretases, but they have failed in clinical trials due to severe side effects or to difficulty in delivery through the blood brain barrier (6–9). Hence, the successful treatments that address the mechanism of modulation of either or both of these APP processing enzymes in Aβ formation remain elusive.

The Receptor for Advanced Glycation of End products (RAGE) is a multiligand member of the immunoglobulin superfamily and functions as a cell surface receptor for Aβ (10–13). Multiple lines of evidence indicate that RAGE is an important cellular cofactor for Aβ-mediated perturbation relevant to the pathogenesis of AD. Investigation of human brains revealed higher levels of RAGE expression in neuronal, microglial and endothelial cells in patients with AD compared with age-matched, non-demented controls (14–18). Expression levels of RAGE are correlated to the severity of the disease indicated by clinical score of the amyloid plaque or tangle (15). Our previous studies on a transgenic mouse model demonstrated elevated expression of RAGE in mice with targeted neuronal overexpression of a mutant form of human APP (mAPP) and increased levels of RAGE in the neurons and microglia of these mice as they age and accumulate Aβ (19,20). Overexpression of RAGE in neurons or microglia of mAPP mice displayed accelerated accumulation of Aβ and exacerbated spatial learning/memory impairment, neuropathological and biochemical changes compared with mAPP mice alone (19,20). On the other hand, introduction of DN-RAGE, signal transduction-deficient mutants of RAGE, into neurons or microglia of mAPP mice exhibited attenuation of Aβ-induced deterioration and displayed preservation of spatial learning/memory and protection against synaptic dysfunction (19–22). These observations suggest that changes of RAGE expression levels might influence the Aβ-induced cellular perturbation relevant to the development and progression of AD. However, the mechanisms of involvement of RAGE in APP processing and Aβ formation have not been elucidated. Additionally, it is unclear whether lack of RAGE would afford protection against cerebral Aβ accumulation and deficits in learning memory in an AD mouse model.

Here, we extended follow-up to our prior studies on the detrimental effects of RAGE-Aβ interaction in AD in order to deepen our comprehensive understanding of the following new questions: 1) Does blockade of RAGE reduce cerebral Aβ accumulation and amyloid pathology together with improvement in cognition? 2) Does RAGE modulate APP processing and subsequent Aβ production? 3) If it does, is RAGE-dependent or independent signaling pathway responsible for activation of β- or γ-secretase? Finally, what may another molecules be involved in this signaling cascade? We generated mAPP mice with genetic deficiency of RAGE (mAPP/RO) and used our previously produced mAPP/DN-RAGE mice targeted to neurons (19), as well as rat neuroblastoma B103-wtAPP cells stably expressing human wild-type (WT) APP (23) to address these key questions. We demonstrated for the first time that deletion or blockade of RAGE or signal transduction-deficient mutants of RAGE confers striking protection from abnormal APP processing and Aβ accumulation. We provided evidence that RAGE-dependent signaling pathway regulates β- and γ-secretase cleavage of APP to generate Aβ, at least in part via activation of glycogen synthase kinase 3β (GSK3β) and p38 MAP kinase.

Results

Effects of RAGE deficiency on Aβ accumulation and β and γ secretase activity in mAPP mice

In view of elevated expression of RAGE correlated to the severity of Aβ accumulation in AD patients and AD mouse model (14–20), we sought to detect the causative effect of RAGE on APP processing and Aβ production by deletion of RAGE in mAPP mice, a well-established animal model for AD. Homozygous RAGE null mice (here termed as RO mice) were crossed with mAPP mice overexpressing mutant APP/Aβ to generate mAPP/RO mice. We demonstrated that RAGE protein levels were significantly elevated in mAPP mice compared with WT mice (Supplementary Material, Fig. S1). In contrast, RAGE expression was blocked in either mAPP/RO or RO mice due to globally genetic deletion of RAGE (Supplementary Material, Fig. S1). Measurement of Aβ by ELISA revealed significantly reduced Aβ40 and Aβ42 levels in the brains of mAPP/RO mice compared with mAPP mice at 12 months of age (Fig. 1A and B). Consistent with these results, quantification of Aβ plaque loads revealed that the area occupied by Aβ deposits in cerebral cortex of mAPP/RO mice was significantly decreased compared with those of mAPP mice at 12 months of age (Fig. 1C and D). Since Aβ is generated from sequential cleavage of APP by β- and γ-secretases, we next examined the effect of RAGE deficiency on APP processing to provide evidence for these two enzyme activities. We performed an *in vitro* cleavage assay, followed by Western blotting to detect the fragments of CTFβ (11 KD) and CTFγ (6 KD) arisen from β- or γ-secretase cleavage of full-length APP that are the indexes of β- and γ-secretase activity, respectively. Notably, the intensity of immunoreactive bands migrating at ∼11 KD and 6 KD corresponding to CTFβ (∼11 KD) and CTFγ (∼6 KD), was significantly reduced by 60% and 50% in mAPP/RO mice, respectively, compared with mAPP mice at 12 months of age (Fig. 1E–G). In parallel, levels of beta-secretase 1 (BACE1), also known as beta-site APP cleaving enzyme 1, was significantly increased in mAPP mouse cortex compared with WT mice, however, it was dramatically reduced in mAPP/RO mice (Fig. 1H). The results of reduced yields of CTFβ and CTFγ as well as decreased BACE1 enzyme in mAPP/RO mice provided the solid evidence that both β- and γ-secretase activities were significantly diminished in mAPP/RO mice compared with mAPP mice. Measurement of endogenous mouse APP in the brain of the four groups of mice (mAPP, mAPP/RO, RO and WT) showed no differences (Fig. 1I). In addition, there are no differences for human APP in mAPP and mAPP/RO mice (Fig. 1J), suggesting that loss of RAGE does not affect APP production. Thus, ablation of RAGE contributes to mitigation of aberrant APP processing and Aβ accumulation via reduction of β- and γ-secretase activity in an AD mouse model.

Effect of RAGE-deficient cytosolic domain in neurons on Aβ production and β- and γ-secretase activity in mAPP mice

Next, we determined whether RAGE had a direct role in transducing signal molecules important for APP cleavage and Aβ production in an Aβ rich environment by employing mAPP/DN-RAGE mice expressing neuronal RAGE-deficient cytosolic domain responsible for RAGE-mediated signal transduction (19). Consistent with our observations on mAPP/RO mice, Aβ40
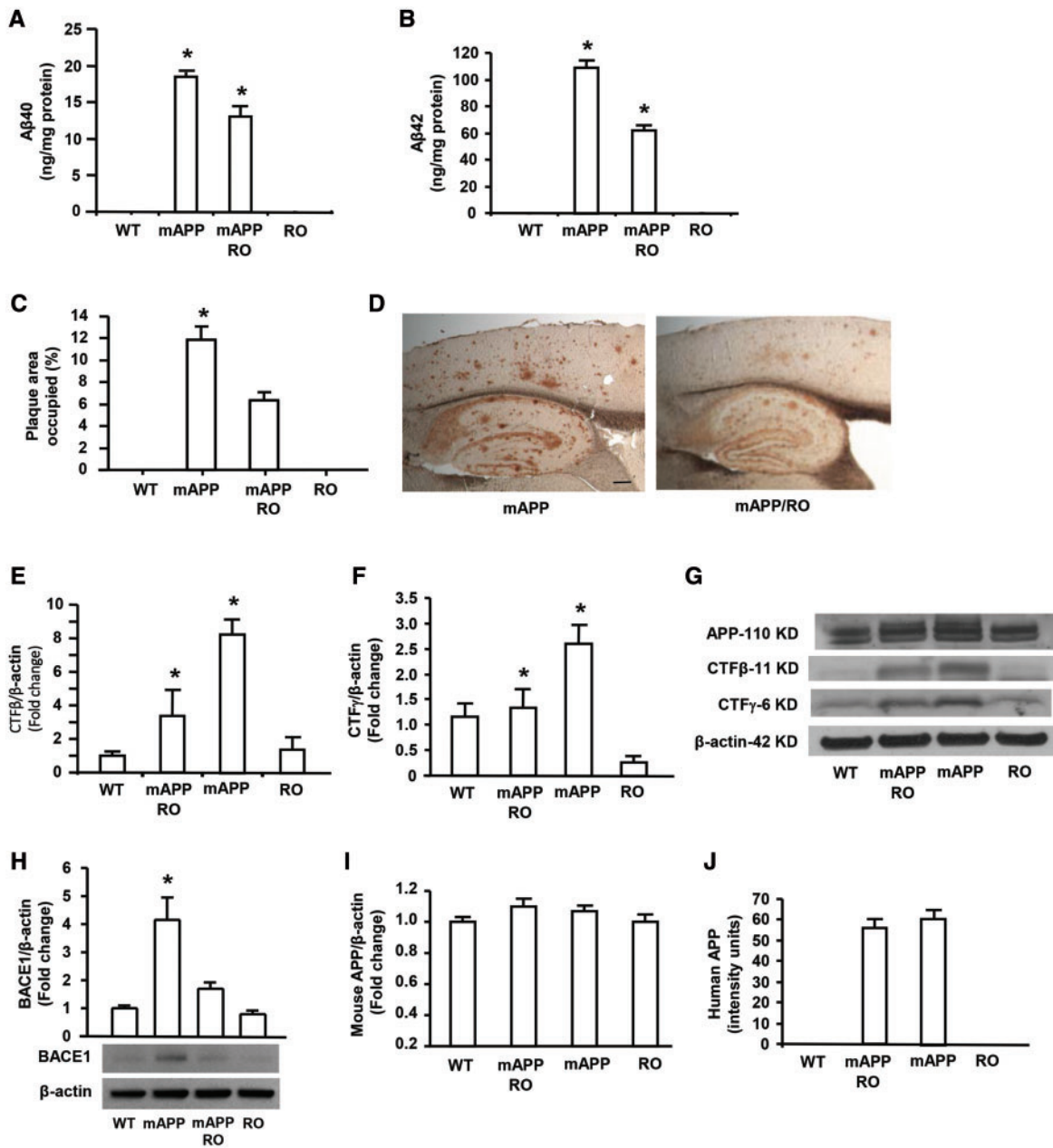
Figure 1. Effect of RAGE deficiency on Aβ accumulation and β and γ secretases activity in mAPP mice. Aβ 40 (**A**) and Aβ 42 (**B**) levels were determined by ELISA in the cortex from 12 month-old mice of the indicated four genotypes ($N = 7$–10 mice/per genotype). Aβ deposits in the cortex (**C**) were quantified by histological image analysis in the brain sections stained with 3D6 antibody in the indicated groups ($N = 5$–10 mice/per genotype). Representative images show the sections stained with 3D6 from mAPP and mAPP/RO mice at 12 months of age (**D**). Scale bar = 30 μm. β- and γ-secretase activity was demonstrated by quantifying intensity of immunoreactive bands of CTFβ (**E**) or CTFγ (**F**) in the brain homogenates from indicated mice. $N = 4$–5 mice/per genotype. Representative immunoblots show immunoreactive bands for APP-110 KD, CTFβ-11 KD and CTFγ-6 KD as well as β-actin protein used as a loading control (**G**). Representative immunoblot and quantitative analysis of immunoreactive band for BACE1 were shown (**H**) and β-actin protein used as a loading control. Quantification of mouse APP (**I**) and human APP (**J**) was performed, respectively. *$P < 0.01$ compared with other groups of mice.

(Fig. 2A) and Aβ42 (Fig. 2B) levels were significantly reduced in the hippocampus homogenates of mAPP/DN-RAGE mice compared with mAPP mice at 10 months of age. The intensity of immunoreactive bands for the fragments of CTFβ and CTFγ generated by β- or γ-secretase cleavage of APP was significantly decreased in mAPP/DN-RAGE mice compared with mAPP mice (Fig. 2C). Accordingly, the intensities of immunoreactive bands for CTFβ and CTFγ were significantly reduced in mAPP/DN-RAGE mice compared with mAPP mice. These data suggest that cytosolic domain of neuronal RAGE signaling is responsible for

aberrant APP processing and Aβ production through magnification of β- and γ-secretase activity in an AD mouse model.

Silencing RAGE gene diminished Aβ production by decreasing β- and γ-secretase activity in human APP/Aβ-producing neuronal cells *in vitro*

To delineate the mechanism underlying the impact of RAGE on regulation of β- and γ-secretase activity, we used rat
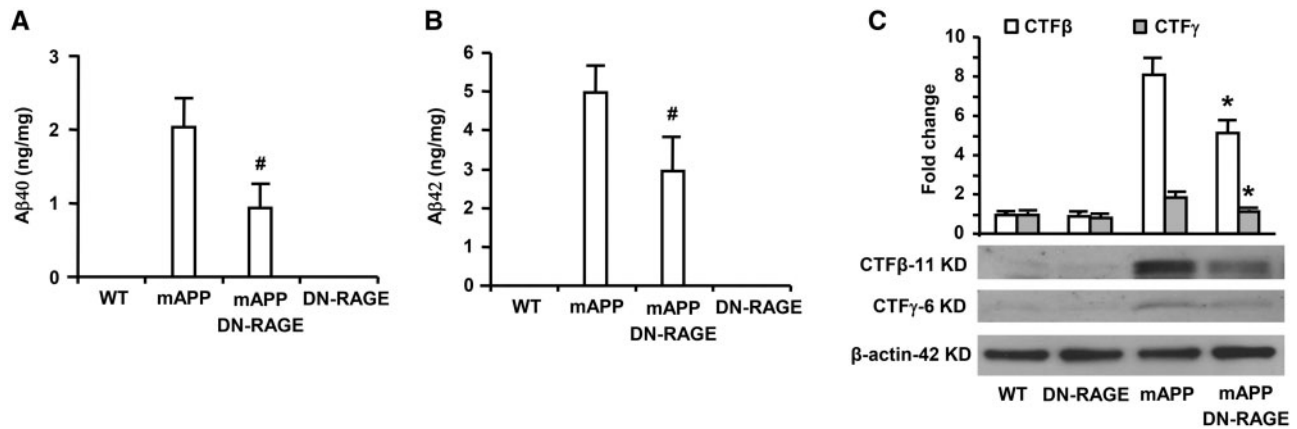
Figure 2. Effect of RAGE-deficient cytosolic domain in neurons on Aβ production and β- and γ-secretase activity in mAPP mice. Aβ40 (**A**) and Aβ42 (**B**) levels in the brain homogenate were determined by ELISA from mice of indicated four genotypes (*N* = 5–7 mice/per genotype). β- and γ-secretase activity was demonstrated by quantifying intensity of immunoreactive bands of CTFβ and CTFγ in brain homogenates from the indicated mice. (**C**) Representative immunoblots show the immunoreactive bands for CTFβ and CTFγ as well as β-actin protein used as a loading control (C). *N* = 4–5 mice/per genotype. #*P* < 0.05 or *P* < 0.01 mAPP/DN-RAGE mice versus mAPP mice.

neuroblastoma B103-wtAPP cells, which stably expressed human APP and were characterized by increase in Aβ fragment production as our *in vitro* model. B103-wtAPP cells were transfected with RAGE siRNA to suppress RAGE expression, and then were assessed for Aβ production and activities of β and γ secretases. First we demonstrated that RAGE mRNA expression by real time quantitative PCR analysis was greatly reduced by ∼80% in B103-wtAPP cells transfected with RAGE siRNA compared with the cells with treatment of non-siRNA or negative control siRNA (Fig. 3A), confirming that RAGE expression was efficiently knockdown by RAGE-siRNA. To investigate Aβ production in RAGE siRNA transfected B103-wtAPP cells, we examined Aβ42 levels in the media and cell lysis of B103-wtAPP cells by ELISA. Knockdown of RAGE by siRNA produced a striking reduction of Aβ42 levels in the media compared with the cells treated with non-siRNA or negative control siRNA (Fig. 3B). Similarly, Aβ42 levels were decreased in the cell lysates of B103-wtAPP cells transfected with RAGE siRNA compared with the cells treated with non-siRNA or negative control siRNA (Fig. 3C). However, Western blot analysis of APP revealed no change in APP cellular level in B103-wtAPP cells after siRNA knockdown of RAGE (Fig. 3D and F). To further investigate the effect of knockdown of RAGE on APP cleavage, B103-wtAPP cells transfected with RAGE siRNA were harvested for assessments of β- and γ-secretase activity. We observed that yields of the fragments of CTFβ and CTFγ were significantly lower in RAGE siRNA transfected B103-wtAPP cells compared with non-siRNA or negative control siRNA transfected cells (Fig. 3E and F), indicating a link of RAGE to APP processing by modulation of both β- and γ-secretase. The negative control siRNA did neither affect APP processing nor alter Aβ levels. These results confirmed specific effects of siRNA knockdown of RAGE gene expression on APP processing and Aβ levels in our experiments. These data suggest that blockage of RAGE reduces β- and γ-secretase cleavage of full-length APP to release Aβ.

Effect of blockade of RAGE-dependent intracellular signaling on Aβ production and β- and γ-secretase activity in human APP/Aβ producing neuronal cells

To further determine the contribution of RAGE-dependent signaling to Aβ production and APP processing, B103-wtAPP cells

were transfected with a DN-RAGE construct. DN-RAGE comprises the extracellular and membrane-spanning domains of RAGE, but lacks the cytosolic tail, which has previously been shown to block RAGE-dependent intracellular signaling mechanism *in vivo* (19,20). *In vitro* analyses, we assessed Aβ production, β- and γ-secretase activity in the above cells. Blockade of RAGE-dependent intracellular signaling in B103-wtAPP cells with DN-RAGE transfection produced a significant reduction of Aβ42 in the media compared with pcDNA3 transfection (Fig. 4A). Accordingly, β- and γ-secretase activity was significantly decreased in DN-RAGE transfected groups compared with pcDNA3 vector transfected groups as evidence by reduction of intensity of immunoreactive bands for these enzymes' decomposition products CTFβ and CTFγ from the full-length of APP (Fig. 4B and D). There were no differences in full length APP in B103-wtAPP cells transfected with DN-RAGE and pcDNA3 (Fig. 4C and D). These data indicate the contribution of RAGE signaling to abnormal APP processing in Aβ milieu. Blockade of RAGE-dependent signaling limits Aβ production by inhibiting activity of β- and γ-secretase, without interfering with APP generation/production.

Effects of RAGE deficiency on activation of GSK3β and p38 signaling pathway in mAPP mice

RAGE functions as a signal transduction receptor, which activates multiple downstream intracellular pathways, including p38 MAP kinase and GSK3 in different disease settings (19,20,22,24–27). Thus, we sought to determine if RAGE mediated cellular activation of such intracellular mechanisms, which might have impact on Aβ production in mAPP mice. Given that GSK3 is a serine/threonine protein kinase and phosphorylation via serine 9 (Ser 9) in the β-isoform inhibits GSK3 activity (28), we tested the phosphorylation of GSK3β (Ser 9) in the indicated groups. Assessment of the phosphorylation levels of GSK3β (Ser 9) revealed a significant lower in mAPP mice than WT control mice at 4 months of age, indicating GSK3β pathway was activated in mAPP mice (Fig. 5A). However, compared with mAPP mice, the increased phosphorylation of GSK3β (Ser 9) leading to its inactivation was observed in mAPP/RO mice (Fig. 5A), indicating that inactivation of GSK3β was evident in mAPP mice devoid of RAGE.
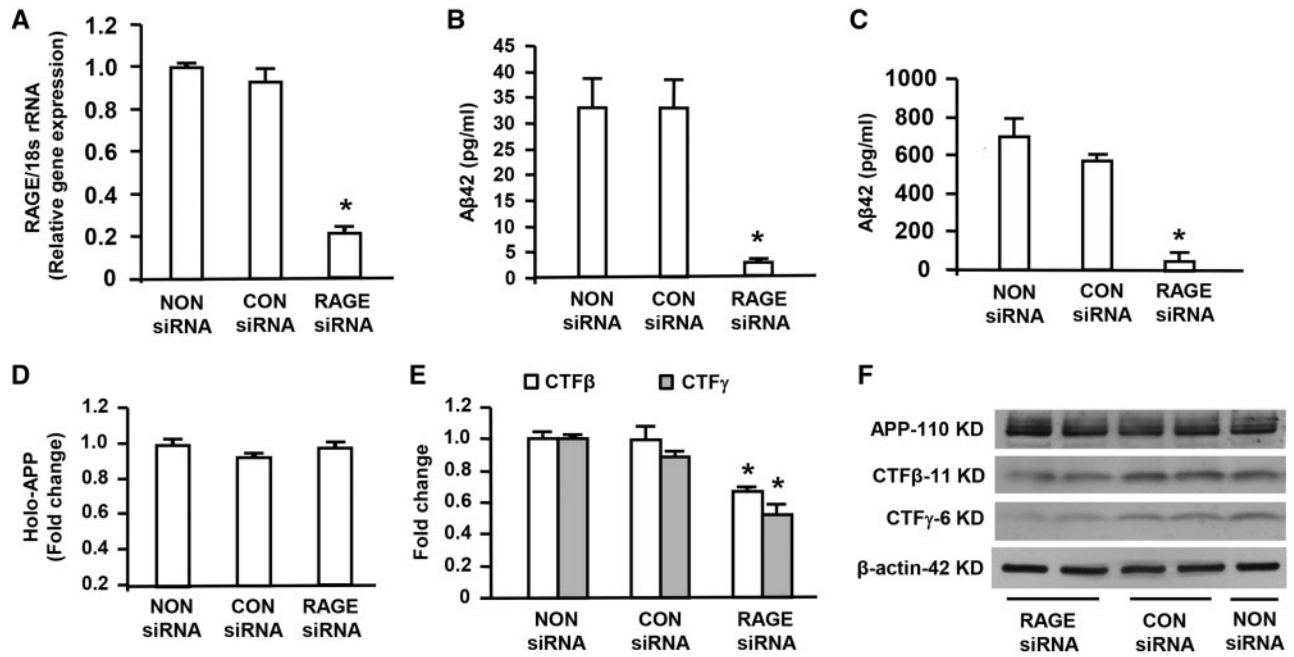
Figure 3. Effect of knockdown of RAGE on Aβ production, β- or γ-secretase activity in human APP/Aβ producing neuronal cells. RNA isolated from B103-wtAPP cells transfected with RAGE siRNA or negative control (CON) siRNA or Non-siRNA was subjected to Real Time PCR analysis of RAGE mRNA levels normalized to 18s rRNA (**A**). Aβ ELISA was used to measure Aβ42 levels in the media (**B**) and cell lysates (**C**) of B103-wtAPP cells transfected with RAGE siRNA or negative control (CON) siRNA or NON-siRNA. Quantification of the immunoreactive bands for APP, CTFβ and CTFγ in B103-wtAPP cells transfected with RAGE siRNA or CON siRNA or NON-siRNA was performed (**D–F**). Representative immunoblots show immunoreactive bands for APP, CTFβ and CTFγ as well as β-actin protein used as a loading control (**F**). Results come from at least three independent experiments. *$P < 0.01$ RAGE siRNA versus CON siRNA or NON siRNA transfected cells.
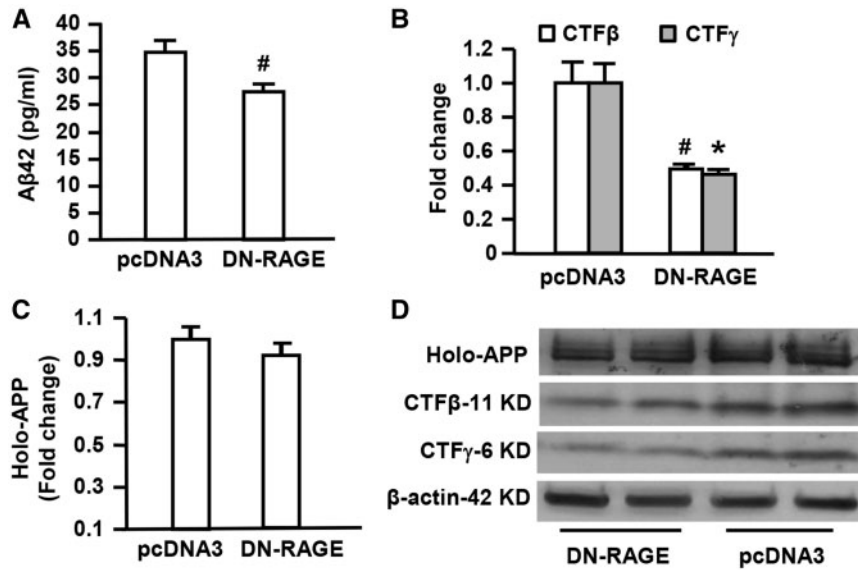

Figure 4. Effect of neuronal RAGE deficient cytosolic domain on Aβ production and β- or γ-secretase activity in human APP/Aβ producing neuronal cells. Aβ ELISA was used for measurement of Aβ42 levels in B103-wtAPP cells transfected with DN-RAGE or pcDNA3 (**A**). Quantification of intensity of immunoreactive bands for APP, CTFβ and CTFγ was performed in B103-wtAPP cells transfected with DN-RAGE or pcDNA3 vector (**B–D**). Representative immunoblots show immunoreactive bands for APP, CTFβ and APP-CTFγ in B103-wtAPP cells transfected with DN-RAGE or pcDNA3 as well as β-actin protein used as a loading control (**D**). Studies were repeated at least three times in each group. #$P < 0.05$ or *$P < 0.01$ DN-RAGE versus pcDNA3 vector-transfected cells.

Given the involvement of RAGE in Aβ-mediated activation of p38 MAP kinase in cultured cortical neurons (25) and neuronal and microglial RAGE overexpressing mAPP mice (19,20), we next determined whether phosphorylated p38 levels were altered *in vivo* Aβ-enriched environment. Indeed, phosphorylation of p38 was elevated in mAPP mice compared with WT mice at 4 months of age (Fig. 5B), which were consistent with our published observations (19,20). Importantly, RAGE-deficient mAPP mice displayed reduction in phosphorylated p38 MAP kinase levels compared with that in mAPP mice (Fig. 5B). These
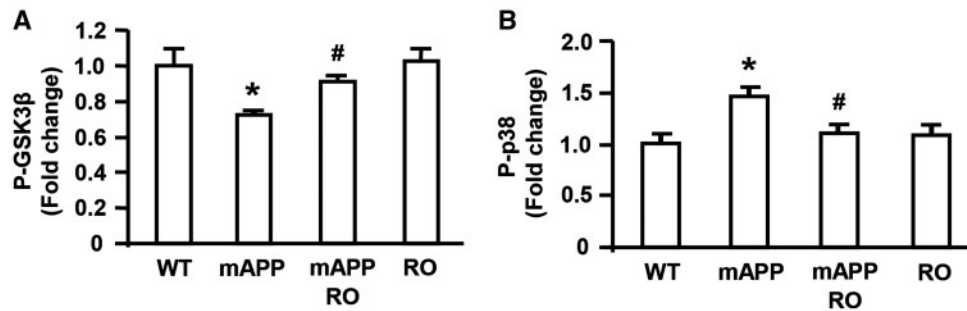
Figure 5. Effect of RAGE deficiency on phosphorylation of GSK3β and p38 MAPK in mAPP mice. The levels of phosphorylated GSK3β at Ser-9 (P-GSK3β) (**A**) and phosphorylated p38 MAPK (**B**) in the mouse brain homogenates from indicated four genotypes were measured by ELISA. The bar graphs show fold increase in phosphorylated GSK3β (A) and phosphorylated p38 MAPK (B), respectively in the brain homogenates from indicated mice. $N = 4$–7 mice per group. *$P < 0.01$ mAPP versus WT mice or RO mice; #$P < 0.05$ mAPP/RO versus mAPP mice.

data demonstrated that lack of RAGE blocks the activation of GSK3β and p38 MAPK signaling pathway in Aβ milieu of mAPP mice.

Effect of inhibition of GSK3β on Aβ production and β- and γ-secretase activity in human APP/Aβ producing neuronal cells

To further determine if RAGE deficiency contributes to lower Aβ production and β- and γ-secretase activity via blockade of activation of GSK3β, lithium chloride (LiCl), a selective inhibitor targeting the inhibitory phosphorylation site of GSK3β (Ser 9), was applied to B103-wtAPP cells. The cells treated with LiCl for 48 h displayed increased phosphorylation of GSK3β (Ser 9) (P-GSK3β) in a dose-dependent manner (Fig. 6A), but without changes in total-GSK3β (T-GSK3β), indicating dose-dependent inhibition of GSK3β activity. Interestingly, addition of SB203580 (1 μM), a specific inhibitor of p38 significantly inhibited GSK3β activation as shown by increased phosphorylated GSK3β (Ser 9) (Fig. 6B). Importantly, similar inhibitory effect on GSK3β activation was observed in DN-RAGE- or RAGE siRNA-transfected B103-wtAPP cells as demonstrated by a significant increase in phosphorylated GSK3β (Ser 9) in DN-RAGE- or RAGE siRNA-transfected B103-wtAPP cells as compared with those control cells transfected with vector or negative control siRNA (Fig. 6C and D). These results provide evidence that blockade or selective deficiency of RAGE signaling or inhibition of p38 phosphorylation hampers activation of GSK3β.

Analogous to RAGE siRNA interference, treatment of LiCl (1 mM) for 48 h, which is able to inhibit GSK3β activity with reduction by 50%, induced significant decrease of Aβ42 production in the medium and cell lysis of B103-wtAPP cells compared with non-treated cells (Fig. 6E and F). In parallel, the intensity of immunoreactive bands for CTFβ and CTFγ fragments were attenuated dramatically in B103-wtAPP cells in the presence of LiCl (1 mM) compared with the absence of LiCl (Fig. 6G), indicating that both β- and γ-secretase activities were significantly decreased by inhibition of GSK3β activity. These findings suggest that GSK3β is a downstream target of p38 and RAGE and its activation plays an important role in regulation of β- and γ-secretase activity in the aberrant APP-Aβ metabolism.

Effect of RAGE deficiency on spatial learning/memory in mAPP mice

Give that progressive deterioration of memory is commonly the presenting complaint in AD, and in view of the early abnormalities of spatial learning/memory in mAPP/RAGE mice overexpressing neuronal or macroglial RAGE but preservation of learning and memory in mAPP/DN-RAGE mice expressing neuronal or microglial signal transduction deficient mutant RAGE compared with mAPP mice (19,20), we investigated whether deletion of RAGE would improve spatial learning and memory in AD mouse model. We evaluated spatial/learning and memory abilities by the radial arm water maze test in mAPP, mAPP/RO, RO mice, and WT littermates. At 12 months of age, mAPP/RO mice displayed significant improvement of spatial learning and memory (~2.5–3 errors by trials 3 and 4 and retention test) compared with mAPP mice (~4–5 errors by trials 3 and 4 and retention test; Fig. 7A). RO mice did not exhibit abnormal behavior compared with WT mice (~2 errors by trials 3 and 4 and retention test). In addition, we also tested mice with a visible platform task to control for motor, sensorial and motivational defects that might have interfered with assessment of mouse behavior during cognitive testing. The four genotypes showed no difference in their latency time and speed to reach the platform and latency to the platform during the visible platform sessions (Fig. 7B and C). These data suggest that RAGE deficiency exerts protective effect on deficits in learning and memory in mice overexpressing mutated APP.

Discussion

Although several important signaling pathways have potential to affect APP proteolysis, we have focused our attention on RAGE-signaling pathway. Our previous studies demonstrated that increased cellular RAGE renders more vulnerable to Aβ-mediated perturbation in patients of AD and in an AD mouse model (15,19,20). However, selective deficiency of neuronal or microglial RAGE signaling by DN-RAGE in the AD mouse model attenuated deterioration induced by Aβ (19–22). Thus, the current study was designed to evaluate whether global deletion of RAGE would have protective effects against Aβ accumulation, amyloid pathology and learning and memory deficits and to elucidate the mechanism by which RAGE regulates β- and γ-secretase activity responsible for cleavage of APP to release Aβ. We developed a genetically modified mouse model (mAPP/RO mice) with deficiency of RAGE (29) in an Aβ-rich environment provided by a transgene for mutant APP/Aβ driven by the PDGF B-chain promoter (30). We demonstrated for the first time that mAPP/RO mice displayed reduced cerebral amyloidosis, inhibited aberrant APP-Aβ metabolism by reducing β- and γ-secretases activity shown as lower yield of CTFβ and CTFγ and less BACE1 enzyme, and attenuated impairment of learning and
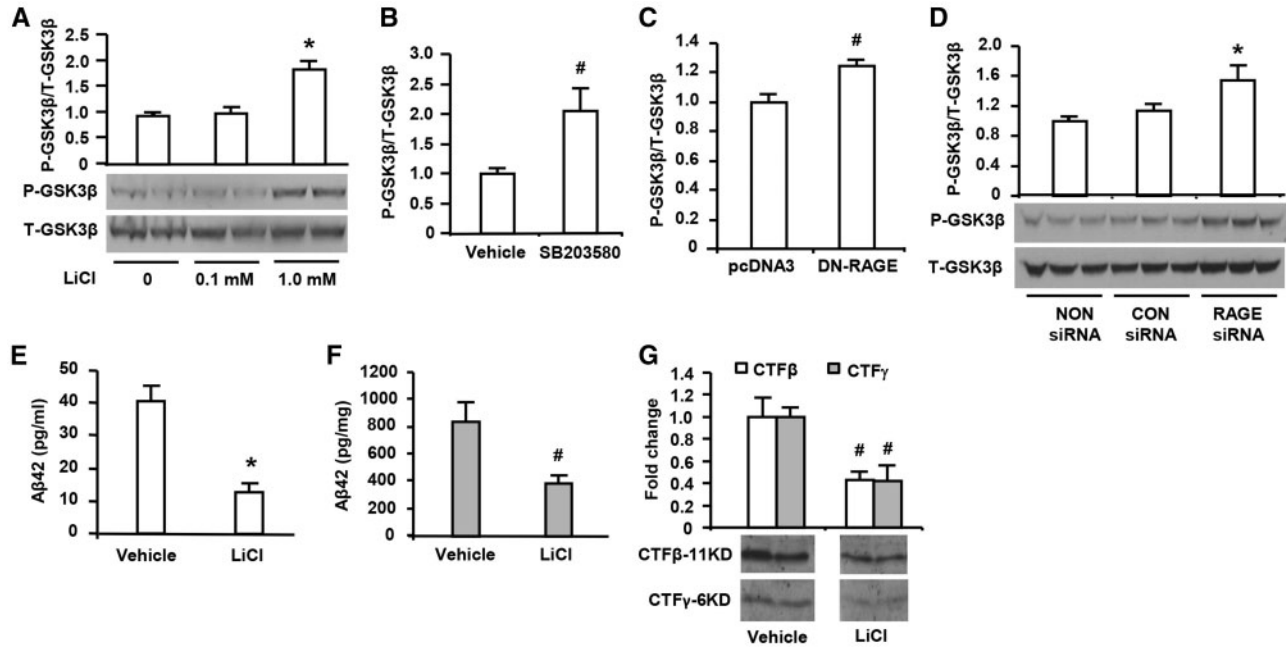
Figure 6. Effect of inhibition of GSK3β on Aβ production and β- and γ-secretase activity in human APP/Aβ producing neuronal cells. Immunoblotting with phosphor-GSK3β (Ser 9) (P-GSK3β) and total GSK3β (T-GSK3β) antibodies were performed in protein extracts from B103-wt APP cells with different treatments. The cells were treated with indicated doses of LiCl for 48 h (**A**,*P < 0.01 versus other groups of cells). The cells were treated with p38 inhibitor SB (203580, 1 μM) for 3 h (**B**, #P < 0.05 p38 inhibitor treated cells versus vehicle-treated cells). The cells were transfected with DN-RAGE 48 h (**C**, #P < 0.05 DN-RAGE versus pcDNA3 vector-transfected cells) and transfected with RAGE siRNA (**D**, *P < 0.01 RAGE siRNA versus CON siRNA or NON siRNA transfected cells). Studies were repeated at least three times in each group. After LiCl (1.0 mM) treatment for 48 h, Aβ42 levels was measured by ELISA in the media (**E**, *P < 0.01 LiCl-treated cells versus vehicle-treated cells) and cell lysates (**F**, #P < 0.05 LiCl treated cells versus vehicle-treated cells) of cultured neuronal cells (B103) stably expressed wild-type APP. Assessment of β- and γ-secretase activity was performed by quantification of intensity of immunoreactive bands for CTFβ and CTFγ (**G**, #P < 0.05 LiCl treated cells versus vehicle-treated cells) in B103-wtAPP cells treated with LiCl. Results come from at least three independent experiments.
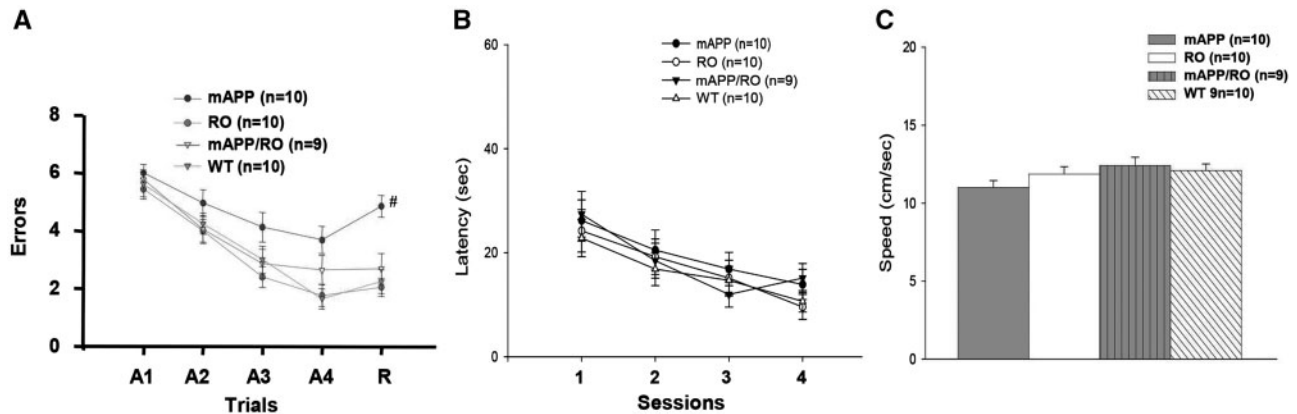

Figure 7. Effect of RAGE deficiency on spatial learning/memory in mAPP mice. Analysis of spatial learning and memory in mAPP/RO mice at 12 months of age using radial arm water maze test, compared with mAPP, RO and WT littermates (**A**) (n = 9–10/group, #P < 0.05). Trials 1–4 acquisition trial and trail 5 denotes retention trail. The four genotypes showed no difference in their latency time (**B**) and speed (**C**) to reach the platform during the visible platform session.

memory compared with mAPP mice at 12 months of age. Importantly, mAPP/DN-RAGE mice expressing neuronal signal transduction deficient mutant RAGE exhibited reduced Aβ40 and Aβ42 production and decreased β-and γ-secretase activity compared with mAPP mice. Further studies on elucidating the potential signal transduction pathways revealed that p38 MAP kinase signaling was significantly down-regulated in the brain of APP/RO mice, and that phosphorylation of GSK3β (Ser 9) was increased in the brain of mAPP/RO mice indicating decreased GSK3β activity by deletion of RAGE, compared with APP mice at early stage 4 months of age. Therefore, we consider these two

pathways as downstream signaling cascades triggered by RAGE that contribute to the early phases of AD based on that activation of p38 MAP kinase and GSK3β was detected in mAPP mice at young age, well before the onset of extensive extracellular Aβ accumulation. Furthermore, suppression of GSK3β activation, inhibition of β- and γ-secretase activity and decrease in Aβ formation by knockdown/blockade of RAGE expression or RAGE-dependent intracellular signaling with RAGE-siRNA/DN-RAGE in the enriched human APP/Aβ neuronal cells provided concrete evidence that RAGE-mediated Aβ formation via GSK3β signaling pathway.
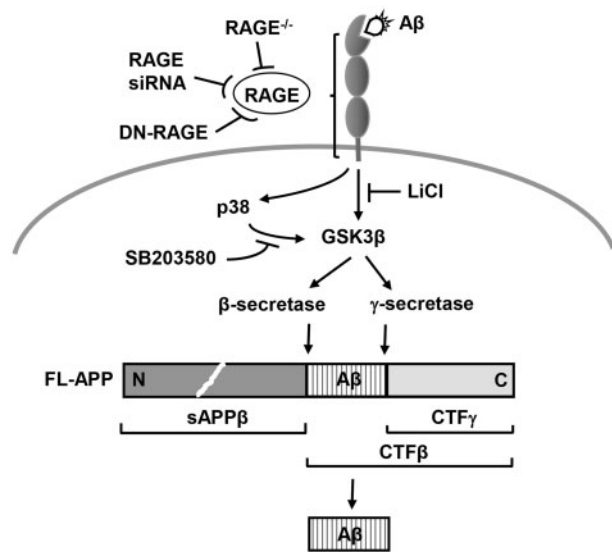
Figure 8. Schematic depiction of RAGE-dependent signaling pathway that regulates β- and γ-secretase cleavage of APP to generate Aβ, at least in part through activation of GSK3β and p38 MAP kinase.

Mounting evidence supports that p38 MAP kinase signaling cascade contributes to cytokine overproduction and neurodegenerative effects seen in AD (20,24,31–33). Activation of p38 MAP kinase was found in early AD brain and in an AD mouse model, while inhibition of p38 MAP kinase activation blocks Aβ-mediated cytokine production and neuronal death (19,20,24,34–36). Our previous studies demonstrated that phosphorylated of p38 levels were significantly increased in mAPP mice compared with WT controls, further, mAPP/RAGE with overexpression of neuronal or microglial RAGE displayed even higher levels of phosphorylated p38 than mAPP mice, whereas mAPP/DN-RAGE exhibited less p38 phosphorylation compared with mAPP mice (19,20). These indicate that existence of RAGE-dependent activation of p38 MAP kinase in neurons and microglia contributes to Aβ-involved neuronal inflammation and neuronal injury. In the current study, we further demonstrated that deficiency of RAGE in mAPP mice significantly mitigated p38 MAP kinase signaling pathway activation accompanying with reduced β- and γ-secretase activity and decreased Aβ production compared with mAPP mice.

RAGE was first identified and characterized as a signal transduction receptor for AGEs (37,38). Methylglyoxal (MG) induced AGEs formation has been reported involving RAGE upregulation and GSK3β activation (27). MG-AGE-induced cardiomyocyte dysfunction was associated with reduced GSK3β inactivation as shown loss of GSK3β (Ser 9) phosphorylation and treatment with RAGE siRNA blocked diabetes-induced GSK3β activation (39). However, involvement of RAGE signaling in regulation of GSK3β activity has not been reported in Aβ-mediated perturbation in AD. GSK3 is widely expressed in all tissues, with particularly abundant levels in brain (40). The widespread expression of GSK3β in the adult brain suggests a fundamental role for GSK3β in neuronal signaling pathways (41). GSK3β has been demonstrated to play an important role in neuronal cell death (42). It has been reported that the neurotoxic effect of Aβ42 is mediated by GSK3β activation, and that inhibition of GSK3β activity can reduce Aβ42-induced neurotoxicity (42), and optimized inhibitor level for modulating GSK3β activity may prevent apoptosis induced by oxidative stress associated with

neurodegenerative diseases (43). LiCl, a selective inhibitor targeting the inhibitory phosphorylation site of GSK3β (Ser 9), was shown to cause a large increase in the phosphorylation of GSK3β (Ser 9) *in vivo* (44), and to protect neurons from apoptosis by inhibiting the activity of GSK3β (45). Specific inhibition of cellular GSK3 by lithium elicits a reduction in Aβ. Indeed, our current results of B103-wtAPP cells showed that LiCl inhibited GSK3β activity in a dose dependent manner with a maximum reduction by 50% and induced significant decrease of Aβ40 and Aβ42 production. Consistent with our observations, lithium inhibited Aβ production was reported in HEK293 cells stably transfected with Swedish (APP)(751) and in the brains of the PDAPP (APP(V717F)) AD transgenic mice (46). Oral administration of lithium abolished GSK3β-mediated Aβ increase in the brains of GSK3β transgenic mice and reduced Aβ plaques burden in the brains of the PDAPP (APP(V717F)) transgenic mice (46). These observations demonstrated that altered GSK3β activity influenced Aβ production levels, suggesting that GSK3β is a potential downstream kinase involved in APP processing. However, these studies lacked the mechanism underlying GSK3β regulation of APP processing. We provided the evidence that inhibition of GSK3β activity in B103-wt APP cells by LiCl significantly attenuated β- and γ-secretase activity as shown lower yield of their cleavage products CTFβ and CTFγ, indicating that β- and γ-secretase is downstream target of GSK3β. Notably, we further demonstrated that deletion of RAGE or neuronal signal transduction deficient mutant RAGE (DN-RAGE) in mAPP mice, or knockdown/blockade of RAGE in B103-wtAPP cells by RAGE-siRNA/DN-RAGE significantly inhibited GSK3β activity accompanying with reduced β- and γ-secretase activity and decreased Aβ production. Our findings indicate that RAGE-dependent signal transduction in GSK3β activation is an important mechanism underlying β- and γ-secretase involved cleavage of APP to generate Aβ (Fig. 8). Moreover, we found that inhibition of p38 phosphorylation significantly suppressed activation of GSK3β, suggesting that GSK3β might be a downstream target of p38 (Fig. 8).

Pharmacological intervention in β- and γ-secretase activity has been heavily investigated for over a decade to prevent the buildup of the amyloid plaques and the formation of toxic amyloid dimmers and oligomers (47). On the basis of the initial studies of ablation of β-secretase (BACE1) in APP-overexpressing mice that demonstrated abolished Aβ generation and no detectable amyloid deposition (48–50), inhibition of the enzymatic activity of BACE1 is considered to be one of the most promising targets for treating AD patients and developing BACE1 inhibitors as therapeutic agents is being energetically pursued. However, the development of β-secretase inhibitor was slowed down because of the difficulty in achieving adequate brain penetration (9). In addition, newly identified BACE1 substrates and deeper analysis of BACE1 null mice that exhibited numerous subtle neuronal phenotypes suggest that complete abolishment of BACE1 activity may result in harmful phenotypical defects in memory processing, myelination and motor coordination (51–53). Moreover, although multiple γ-secretase inhibitors have been reported to reduce Aβ production both *in vitro* and *in vivo* (54–59), and improve cognitive functioning in a transgenic mouse model of AD (60), active γ-secretase inhibitors investigated in clinic but Phase III trial with semagacestat was prematurely halted in 2010 because of decline in cognition and increase risk of skin cancer (61). Then, the γ-secretase research has fallen into disgrace due to that failed γ-secretase inhibitor Alzheimer's clinical trial led to abrupt closure of promising lines of γ-secretase work (7). Therefore, the successful treatments

that address the mechanism of modulation of either or both of these APP processing enzymes in Aβ formation are urgent need. Our present findings suggest that blockade/inhibition of RAGE may offer a new approach to reduce Aβ formation by modulating β- and γ-secretase cleavage of APP to halt progression of AD.

In summary, the data presented herein clearly demonstrated, for the first time, that genetic deficiency of RAGE significantly reduced Aβ accumulation in the brain by modulating β- and γ-secretase activity through GSK-3β and p38 signaling pathway and improved spatial learning and memory in an AD mouse model. Our findings suggest that RAGE is a potential target to limit aberrant APP-Aβ metabolism in halting progression of AD.

Materials and Methods

Generation and characterization of genetically modified mice

Transgenic mice with neuronal overexpression of a mutant human form of APP (Tg mAPP or mAPP, J-20 line, Jackson Lab) driven by the platelet-derived growth factor (PDGF) B-chain promoter were used in this study (30). These mAPP mice are a well-established mouse model of AD and exhibit many features of AD neuropathology (19,30), and have been used in previously published studies (19,20,62–65). Homozygous RAGE null mice (29) (here termed as RO mice) were backcrossed into C57BL/6 strain for more than 12 generations, and were crossed with mAPP mice to generate mAPP/RO *mice*. The mAPP/DN-RAGE mice were produced in our laboratory as previously published (19). Age- and sex-matched non-genetically modified WT littermates were used as controls in our studies. Mice were maintained on normal rodent chow and allowed free access to food and water at all times. Genomic DNA was isolated from tail biopsies and subjected to PCR analysis to identify the deficiency of RAGE or the presence of DN-RAGE or human APP gene.

The mice were anesthetized with ketamine (100 mg/kg) and xylazine (10 mg/kg) and flush perfused transcardially with 0.9% saline. Brains were removed and divided sagittally. One hemibrain was post-fixed in phosphate-buffered 4% paraformaldehyde (pH 7.4) at 4°C for 26 h and sectioned at 20 μm with a Vibratome (Leica); the other hemibrain was dissected to hippocampus and cortex, snap frozen and stored at –80°C for protein analysis and Aβ ELISA. All animal studies were carried out with the approval of the Institutional Animal Care and Use Committee of Columbia University and University of Kansas.

Cell cultures

Rat neuroblastoma B103 cells stably expressing human WT APP were kindly provided by Tony Wyss-Coray (23). B103-wtAPP cells were maintained in Dulbecco's modified Eagle's medium (DMEM, Catalog #10313021; Invitrogen/Thermo Fisher Scientific, Austin, TX, USA) containing 10% FBS, 5% heat inactivated horse serum, 500 μg/ml G418 (Catalog #11811023; Thermo Fisher Scientific, Austin, TX, USA). Cells were washed with serum free DMEM 24 h after planting and cultured in neurobasal medium containing 1% N-2 supplement (Catalog # 17502048, Thermo Fisher Scientific, Austin, TX, USA) to induce differentiation.

Transfection

B103-wtAPP cells were transfected with rat RAGE siRNA using siPORT Amine according to the manufacturer's pre-plate transfection procedure. Rat RAGE siRNA (Catalog #81722; ID s135582), negative control siRNA #4 (Catalog #AM4641) and siPORT Amine (Catalog #AM4641) were purchased from Applied Biosystems/Thermo Fisher Scientific (Austin, TX, USA). Briefly, cells were seeded on 6-well plates with normal growth medium so that they reached by 80% confluence after 24 h. SiPORT Amine agent was diluted into OPTI-MEM I medium (Catalog #11058021, Thermo Fisher Scientific) and incubated for 10 min at room temperature. Combine the diluted siPORT Amine with the diluted siRNA by pipetting up and down. Incubate 10 min at room temperature to allow transfection complexes to form. Mix the transfection complexes with cells and incubate at 37°C. Add equal amount of normal growth medium containing 20% FBS to the wells after 4 h. After 48 h, cells were harvested for RNA isolation using TRIZOL (Catalog #15596-018, Invitrogen/Thermo Fisher Scientific) or for protein expression analysis using lysis buffer.

Real-time quantitative PCR

Real-time quantitative PCR was performed as previously described (20). Briefly, total RNA from transfected and non-transfected B103-wtAPP cells was isolated using TRIZOL and was processed directly to cDNA synthesis using the TaqMan reverse transcription reagents Kit (Catalog #N808-0234) from Applied Biosystems/Thermo Fisher Scientific (Austin, TX, USA) according to the manufacturer's protocol. Real-time PCR was performed using TaqMan Universal PCR Master Mix (Catalog #4304437, Applied Biosystems/Thermo Fisher Scientific, Austin, TX, USA). The rat RAGE (Catalog #4331182, ID #Rn00584249_m1) and ribosomal RNA (18s rRNA) probes and primers were purchased from Applied Biosystems/Thermo Fisher Scientific (Austin, TX, USA). Data are calculated using the $2^{-\Delta\Delta Ct}$ method (66) and are presented as fold reduction of transcripts for target genes in RAGE siRNA transfected B103-wtAPP cells normalized to 18s rRNA, compared with control siRNA transfected B103-wtAPP cells (defined as 1.0-fold in each case). All reactions were performed in triplicate in ABI PRISM 7900HT Sequence Detection System.

Western blotting

Total protein extracts were prepared from the dissected frontal cortical brain from snap-frozen hemi-brains by homogenization with 1× RIPA buffer (Catalog #9806, Cell Signaling Technology, MA) containing 1× protease inhibitor cocktail (Roche Applied Science, IN) and 1 mM PMSF. Total protein extracts from B103-wtAPP cells were prepared using 1× cell lysis buffer (Catalog #9803, Cell Signaling Technology, MA) containing 1× protease inhibitor cocktail and 1 mM PMSF. Protein concentrations of the tissue or cell lysates were determined with Bio-Rad protein assay kit. The equal amount of protein from each sample was separated by SDS/PAGE (10% Bis–Tris gel, Catalog# NP0301, Invitrogen/Thermo Fisher Scientific, Austin, USA), and then electrophoretically transferred to 0.45 μm nitrocellular membranes (Catlog# 162-0094, Bio-Rad Laboratories, Hercules, CA, USA). Non-specific binding was blocked by 5% non-fat milk in TBS buffer (20 mM Tris–HCl, 150 mM NaCl, pH 7.6) for 1 h at room temperature. The membrane was incubated in diluted primary antibody in TBST (TBS containing 0.1% Tween-20, pH 7.6) overnight with gentle shaking at 4°C. The primary antibodies used for the reactions were as follows: rabbit anti-RAGE (1:1000, house-made), rabbit anti-BACE1 (1:3000, Catalog #ab108394,

Abcam, Cambridge, UK), rabbit anti-Phospho-GSK3β (Ser9) (P-GSK3β) and Total-GSK3 β (1:3000; Catalog #9336 and #9315, Cell signaling Technology, MA), mouse anti-β-actin (1:5000, Catalog #A5441, Sigma, St. Louis, MO, USA). The membrane was washed with TBST and then incubated with the corresponding horse-radish peroxidase-conjugated secondary antibody: goat anti-rabbit IgG or goat anti-mouse (1:10 000, Catalog #A6154 or #A4416, Sigma, St. Louis, MO, USA), for 1 h with gentle shaking at room temperature to identify sites of binding of each primary antibody. Finally, the chemiluminescent signal from immunor-eactive band was detected using an enhanced chemilumines-cent Western blot system (GE Healthcare, NJ). The signals were quantified by Image J (NIH).

In vitro cleavage assay for assessment of β- and γ-secretase activity

Freshly dissected mouse cerebral cortex was homogenized in homogenization buffer (10 mM MOPS, pH 7.0, 10 mM KCl, 1× complete protease inhibitor cocktail) and centrifuge at 2500 rpm for 15 min at 4°C. The supernatant was collected and centrifuged at 14 000 rpm for 20 min at 4°C. The pellet was rinsed once with homogenization buffer and then resuspended in assay buffer (150 mM sodium citrate, pH 6.4, 1× complete protease inhibitor cocktail, protein concentration 4 μg/μl). The reaction mixtures were incubated at 37°C for 2 h. The fragments of CTFβ (∼11 KD) and CTFγ (∼6 KD) arisen from β- and γ-secretase cleavage of full-length APP were detected by Western blotting using 10–20% Tricine gels (Invitrogen/Thermo Fisher Scientific, Austin, TX, USA), 0.2 μm Nitrocellulose membrane (Catalog# 1620112, Bio-Rad Laboratories, Hercules, CA, USA), and anti-APP-CTF anti-body (Catalog #171610, Calbiochem, MA). The full-length APP was also detected by Western blot with anti-APP-CTF antibody. B103-wtAPP neuroblastoma cells transfected with RAGE siRNA or DN-RAGE or treated with LiCl were washed with cold 1× PBS twice before being harvested with homogenization buffer and then processed the same as tissue samples. APP, CTFβ and CTFγ signals were visualized by enhanced chemiluminescence (GE Healthcare, NJ) and exposure to X-ray film, scanned with a HP scanner and quantified by Image J (NIH).

ELISA

Aβ ELISA analysis was performed to measure total human Aβ40 and Aβ42 levels in the brain tissue of the genetically modified mice and non-genetically modified WT littermates as previously described (19,63–65,67–69). The brain tissue was extracted with 8 volumes of guanidine–Tris buffer (5.0 M Guanidine HCl/50 mM Tris–HCl, pH 8.0). B103-wtAPP neuroblastoma cells were also lysed in 5.0 M guanidine–Tris buffer. The homogenates were mixed at room temperature for 3–4 h and then subjected to sandwich ELISA to measure the specific human Aβ40 and human Aβ42 according to the manufacturer's instructions (Catalog #KHB3482 and #KHB3442; Invitrogen/Thermo Fisher Scientific, Austin, TX, USA). Aβ42 levels in conditioned media of B103-wtAPP cells were also detected by Invitrogen human Aβ 42 ELISA kits. Phosphorylation of GSK3β and p38 in mouse brain homogenates were determined by using GSK3β [pS9] ELISA Kit and p38 MAPK [pTpY180/182] phosphoELISA™ Kit according to manufacturer's protocol (Catalog #KHO0461 and #KHO0071 Invitrogen/Thermo Fisher Scientific, Austin, TX, USA).

Histochemical analyses

Serial vibratome sections (20 μm) were cut from 4% paraformaldehyde-fixed mice brains. Immunocytochemical analyses were performed using anti-Aβ antibody 3D6 (dilution 1:1000, provided by Eli Lilly, Indianapolis, IN, USA) to identify Aβ deposits. The area occupied by amyloid plaques in the entire hippocampus and cortex from the same level section in each animal group was determined by image analysis, using MetaMorph software from Universal Imaging Corporation (West Chester, PA).

Behavioral studies

Behavioral studies were performed to assess spatial learning and memory in the radial arm water maze as previously described (19). The investigators were blinded to mouse geno-types until behavioral testing was completed.

Statistical analysis

All data are presented as means ± SEM. Statistical comparisons between different groups were performed with ANOVA for repeated measure analysis using commercially available soft-ware (Statview, version 5.0.1, Berkeley, CA), followed by Fisher's protected least significant difference for post hoc comparisons. $P \leq 0.05$ was considered significant.

Supplementary Material

Supplementary Material is available at *HMG* online.

Conflict of Interest statement. None declared.

References

1. Selkoe, D.J. (1999) Translating cell biology into therapeutic advances in Alzheimer's disease. *Nature*, **399**, A23–A31.
2. Vassar, R. and Citron, M. (2000) Abeta-generating enzymes: recent advances in beta- and gamma-secretase research. *Neuron*, **27**, 419–422.
3. Nunan, J., Shearman, M.S., Checler, F., Cappai, R., Evin, G., Beyreuther, K., Masters, C.L. and Small, D.H. (2001) The C-terminal fragment of the Alzheimer's disease amyloid protein precursor is degraded by a proteasome-dependent mechanism distinct from gamma-secretase. *Eur. J. Biochem.*, **268**, 5329–5336.
4. Chang, Y., Tesco, G., Jeong, W.J., Lindsley, L., Eckman, E.A., Eckman, C.B., Tanzi, R.E. and Guenette, S.Y. (2003) Generation of the beta-amyloid peptide and the amyloid precursor protein C-terminal fragment gamma are potenti-ated by FE65L1. *J. Biol. Chem.*, **278**, 51100–51107.
5. O'Brien, R.J. and Wong, P.C. (2011) Amyloid precursor protein processing and Alzheimer's disease. *Ann. Rev. Neurosci.*, **34**, 185–204.
6. De Strooper, B. (2010) Proteases and proteolysis in Alzheimer disease: a multifactorial view on the disease process. *Physiol. Rev.*, **90**, 465–494.

7. Doody, R.S., Raman, R., Farlow, M., Iwatsubo, T., Vellas, B., Joffe, S., Kieburtz, K., He, F., Sun, X., Thomas, R.G. *et al.* (2013) A phase 3 trial of semagacestat for treatment of Alzheimer's disease. *N. Engl. J. Med.*, **369**, 341–350.

8. De Strooper, B. (2014) Lessons from a failed gamma-secretase Alzheimer trial. *Cell*, **159**, 721–726.

9. Zimmermann, M., Gardoni, F. and Di Luca, M. (2005) Molecular rationale for the pharmacological treatment of Alzheimer's disease. *Drugs Aging*, **22(Suppl. 1)**, 27–37.

10. Bierhaus, A., Humpert, P.M., Morcos, M., Wendt, T., Chavakis, T., Arnold, B., Stern, D.M. and Nawroth, P.P. (2005) Understanding RAGE, the receptor for advanced glycation end products. *J. Mol. Med. (Berlin, Germany)*, **83**, 876–886.

11. Schmidt, A.M., Yan, S.D., Yan, S.F. and Stern, D.M. (2001) The multiligand receptor RAGE as a progression factor amplifying immune and inflammatory responses. *J. Clin. Investig.*, **108**, 949–955.

12. Yan, S.D., Yan, S.F., Chen, X., Fu, J., Chen, M., Kuppusamy, P., Smith, M.A., Perry, G., Godman, G.C., Nawroth, P. *et al.* (1995) Non-enzymatically glycated tau in Alzheimer's disease induces neuronal oxidant stress resulting in cytokine gene expression and release of amyloid beta-peptide. *Nat. Med.*, **1**, 693–699.

13. Yan, S.D., Bierhaus, A., Nawroth, P.P., Stern, D.M. and Bierhaus, A. (2009) RAGE and Alzheimer's disease: a progression factor for amyloid-beta-induced cellular perturbation? *J. Alzheimer's Dis.: JAD*, **16**, 833–843.

14. Yan, S.D., Chen, X., Fu, J., Chen, M., Zhu, H., Roher, A., Slattery, T., Zhao, L., Nagashima, M., Morser, J. *et al.* (1996) RAGE and amyloid-beta peptide neurotoxicity in Alzheimer's disease. *Nature*, **382**, 685–691.

15. Lue, L.F., Walker, D.G., Brachova, L., Beach, T.G., Rogers, J., Schmidt, A.M., Stern, D.M. and Yan, S.D. (2001) Involvement of microglial receptor for advanced glycation endproducts (RAGE) in Alzheimer's disease: identification of a cellular activation mechanism. *Exp. Neurol.*, **171**, 29–45.

16. Sasaki, N., Toki, S., Chowei, H., Saito, T., Nakano, N., Hayashi, Y., Takeuchi, M. and Makita, Z. (2001) Immunohistochemical distribution of the receptor for advanced glycation end products in neurons and astrocytes in Alzheimer's disease. *Brain Res.*, **888**, 256–262.

17. Miller, M.C., Tavares, R., Johanson, C.E., Hovanesian, V., Donahue, J.E., Gonzalez, L., Silverberg, G.D. and Stopa, E.G. (2008) Hippocampal RAGE immunoreactivity in early and advanced Alzheimer's disease. *Brain Res.*, **1230**, 273–280.

18. Yan, S.S., Chen, D., Yan, S., Guo, L., Du, H. and Chen, J.X. (2012) RAGE is a key cellular target for Abeta-induced perturbation in Alzheimer's disease. *Front. Biosci. (Sch. Ed.)*, **4**, 240–250.

19. Arancio, O., Zhang, H.P., Chen, X., Lin, C., Trinchese, F., Puzzo, D., Liu, S., Hegde, A., Yan, S.F., Stern, A. *et al.* (2004) RAGE potentiates Abeta-induced perturbation of neuronal function in transgenic mice. *EMBO J.*, **23**, 4096–4105.

20. Fang, F., Lue, L.F., Yan, S., Xu, H., Luddy, J.S., Chen, D., Walker, D.G., Stern, D.M., Yan, S., Schmidt, A.M. *et al.* (2010) RAGE-dependent signaling in microglia contributes to neuroinflammation, Abeta accumulation, and impaired learning/memory in a mouse model of Alzheimer's disease. *FASEB J.*, **24**, 1043–1055.

21. Criscuolo, C., Fontebasso, V., Middei, S., Stazi, M., Ammassari-Teule, M., Yan, S.S. and Origlia, N. (2017) Entorhinal Cortex dysfunction can be rescued by inhibition of microglial RAGE in an Alzheimer's disease mouse model. *Sci. Rep.*, **7**, 42370.

22. Origlia, N., Criscuolo, C., Arancio, O., Yan, S.S. and Domenici, L. (2014) RAGE inhibition in microglia prevents ischemia-dependent synaptic dysfunction in an amyloid-enriched environment. *J. Neurosci.*, **34**, 8749–8760.

23. Tesseur, I., Zou, K., Esposito, L., Bard, F., Berber, E., Can, J.V., Lin, A.H., Crews, L., Tremblay, P., Mathews, P. *et al.* (2006) Deficiency in neuronal TGF-beta signaling promotes neurodegeneration and Alzheimer's pathology. *J. Clin. Investig.*, **116**, 3060–3069.

24. Origlia, N., Righi, M., Capsoni, S., Cattaneo, A., Fang, F., Stern, D.M., Chen, J.X., Schmidt, A.M., Arancio, O., Yan, S.D. *et al.* (2008) Receptor for advanced glycation end product-dependent activation of p38 mitogen-activated protein kinase contributes to amyloid-beta-mediated cortical synaptic dysfunction. *J. Neurosci.*, **28**, 3521–3530.

25. Takuma, K., Fang, F., Zhang, W., Yan, S., Fukuzaki, E., Du, H., Sosunov, A., McKhann, G., Funatsu, Y., Nakamichi, N. *et al.* (2009) RAGE-mediated signaling contributes to intraneuronal transport of amyloid-beta and neuronal dysfunction. *Proc. Natl. Acad. Sci. U. S. A.*, **106**, 20021–20026.

26. Zhang, H., Wang, Y., Yan, S., Du, F., Wu, L., Yan, S. and Yan, S.S. (2014) Genetic deficiency of neuronal RAGE protects against AGE-induced synaptic injury. *Cell Death Dis.*, **5**, e1288.

27. Li, X.H., Xie, J.Z., Jiang, X., Lv, B.L., Cheng, X.S., Du, L.L., Zhang, J.Y., Wang, J.Z. and Zhou, X.W. (2012) Methylglyoxal induces tau hyperphosphorylation via promoting AGEs formation. *Neuromol. Med.*, **14**, 338–348.

28. Stambolic, V. and Woodgett, J.R. (1994) Mitogen inactivation of glycogen synthase kinase-3 beta in intact cells via serine 9 phosphorylation. *Biochem. J.*, **303**, 701–704.

29. Sakaguchi, T., Yan, S.F., Yan, S.D., Belov, D., Rong, L.L., Sousa, M., Andrassy, M., Marso, S.P., Duda, S., Arnold, B. *et al.* (2003) Central role of RAGE-dependent neointimal expansion in arterial restenosis. *J. Clin. Investig.*, **111**, 959–972.

30. Mucke, L., Masliah, E., Yu, G.Q., Mallory, M., Rockenstein, E.M., Tatsuno, G., Hu, K., Kholodenko, D., Johnson-Wood, K. and McConlogue, L. (2000) High-level neuronal expression of abeta 1-42 in wild-type human amyloid protein precursor transgenic mice: synaptotoxicity without plaque formation. *J. Neurosci.*, **20**, 4050–4058.

31. Johnson, G.V. and Bailey, C.D. (2003) The p38 MAP kinase signaling pathway in Alzheimer's disease. *Exp. Neurol.*, **183**, 263–268.

32. Kim, E.K. and Choi, E.J. (2010) Pathological roles of MAPK signaling pathways in human diseases. *Biochim. Biophys. Acta*, **1802**, 396–405.

33. Hensley, K., Floyd, R.A., Zheng, N.Y., Nael, R., Robinson, K.A., Nguyen, X., Pye, Q.N., Stewart, C.A., Geddes, J., Markesbery, W.R. *et al.* (1999) p38 kinase is activated in the Alzheimer's disease brain. *J. Neurochem.*, **72**, 2053–2058.

34. Munoz, L., Ralay Ranaivo, H., Roy, S.M., Hu, W., Craft, J.M., McNamara, L.K., Chico, L.W., Van Eldik, L.J. and Watterson, D.M. (2007) A novel p38 alpha MAPK inhibitor suppresses brain proinflammatory cytokine up-regulation and attenuates synaptic dysfunction and behavioral deficits in an Alzheimer's disease mouse model. *J. Neuroinflammation*, **4**, 21.

35. Zhu, X., Mei, M., Lee, H.G., Wang, Y., Han, J., Perry, G. and Smith, M.A. (2005) P38 activation mediates amyloid-beta cytotoxicity. *Neurochem. Res.*, **30**, 791–796.

36. Pyo, H., Jou, I., Jung, S., Hong, S. and Joe, E.H. (1998) Mitogen-activated protein kinases activated by lipopolysaccharide and beta-amyloid in cultured rat microglia. *Neuroreport*, **9**, 871–874.

37. Schmidt, A.M., Vianna, M., Gerlach, M., Brett, J., Ryan, J., Kao, J., Esposito, C., Hegarty, H., Hurley, W., Clauss, M. *et al.* (1992) Isolation and characterization of two binding proteins for advanced glycosylation end products from bovine lung which are present on the endothelial cell surface. *J. Biol. Chem.*, **267**, 14987–14997.

38. Neeper, M., Schmidt, A.M., Brett, J., Yan, S.D., Wang, F., Pan, Y.C., Elliston, K., Stern, D. and Shaw, A. (1992) Cloning and expression of a cell surface receptor for advanced glycosylation end products of proteins. *J. Biol. Chem.*, **267**, 14998–15004.

39. Ma, H., Li, S.Y., Xu, P., Babcock, S.A., Dolence, E.K., Brownlee, M., Li, J. and Ren, J. (2009) Advanced glycation endproduct (AGE) accumulation and AGE receptor (RAGE) up-regulation contribute to the onset of diabetic cardiomyopathy. *J. Cell. Mol. Med.*, **13**, 1751–1764.

40. Woodgett, J.R. (1990) Molecular cloning and expression of glycogen synthase kinase-3/factor A. *EMBO J.*, **9**, 2431–2438.

41. Leroy, K. and Brion, J.P. (1999) Developmental expression and localization of glycogen synthase kinase-3beta in rat brain. *J. Chem. Neuroanat.*, **16**, 279–293.

42. Koh, S.H., Noh, M.Y. and Kim, S.H. (2008) Amyloid-beta-induced neurotoxicity is reduced by inhibition of glycogen synthase kinase-3. *Brain Res.*, **1188**, 254–262.

43. Lee, K.Y., Koh, S.H., Noh, M.Y., Park, K.W., Lee, Y.J. and Kim, S.H. (2007) Glycogen synthase kinase-3beta activity plays very important roles in determining the fate of oxidative stress-inflicted neuronal cells. *Brain Res.*, **1129**, 89–99.

44. De Sarno, P., Li, X. and Jope, R.S. (2002) Regulation of Akt and glycogen synthase kinase-3 beta phosphorylation by sodium valproate and lithium. *Neuropharmacology*, **43**, 1158–1164.

45. Bijur, G.N., De Sarno, P. and Jope, R.S. (2000) Glycogen synthase kinase-3beta facilitates staurosporine- and heat shock-induced apoptosis. Protection by lithium. *J. Biol. Chem.*, **275**, 7583–7590.

46. Su, Y., Ryder, J., Li, B., Wu, X., Fox, N., Solenberg, P., Brune, K., Paul, S., Zhou, Y., Liu, F. *et al.* (2004) Lithium, a common drug for bipolar disorder treatment, regulates amyloid-beta precursor protein processing. *Biochemistry*, **43**, 6899–6908.

47. De Strooper, B., Vassar, R. and Golde, T. (2010) The secretases: enzymes with therapeutic potential in Alzheimer disease. *Nat. Rev. Neurol.*, **6**, 99–107.

48. Luo, Y., Bolon, B., Kahn, S., Bennett, B.D., Babu-Khan, S., Denis, P., Fan, W., Kha, H., Zhang, J., Gong, Y. *et al.* (2001) Mice deficient in BACE1, the Alzheimer's beta-secretase, have normal phenotype and abolished beta-amyloid generation. *Nature Neurosci.*, **4**, 231–232.

49. Cai, H., Wang, Y., McCarthy, D., Wen, H., Borchelt, D.R., Price, D.L. and Wong, P.C. (2001) BACE1 is the major beta-secretase for generation of Abeta peptides by neurons. *Nat. Neurosci.*, **4**, 233–234.

50. Roberds, S.L., Anderson, J., Basi, G., Bienkowski, M.J., Branstetter, D.G., Chen, K.S., Freedman, S.B., Frigon, N.L., Games, D., Hu, K. *et al.* (2001) BACE knockout mice are healthy despite lacking the primary beta-secretase activity in brain: implications for Alzheimer's disease therapeutics. *Hum. Mol. Genet.*, **10**, 1317–1324.

51. Hu, X., Zhou, X., He, W., Yang, J., Xiong, W., Wong, P., Wilson, C.G. and Yan, R. (2010) BACE1 deficiency causes altered neuronal activity and neurodegeneration. *J. Neurosci.*, **30**, 8819–8829.

52. Menting, K.W. and Claassen, J.A. (2014) beta-secretase inhibitor; a promising novel therapeutic drug in Alzheimer's disease. *Front. Aging Neurosci.*, **6**, 165.

53. Vassar, R. (2014) BACE1 inhibitor drugs in clinical trials for Alzheimer's disease. *Alzheimer's Res. Therapy*, **6**, 89.

54. Dovey, H.F., John, V., Anderson, J.P., Chen, L.Z., de Saint Andrieu, P., Fang, L.Y., Freedman, S.B., Folmer, B., Goldbach, E., Holsztynska, E.J. *et al.* (2009) Functional gamma-secretase inhibitors reduce beta-amyloid peptide levels in brain. *J. Neurochem.*, **76**, 173–181.

55. Jack, C., Berezovska, O., Wolfe, M.S. and Hyman, B.T. (2001) Effect of PS1 deficiency and an APP gamma-secretase inhibitor on Notch1 signaling in primary mammalian neurons. *Brain Res. Mol. Brain Res.*, **87**, 166–174.

56. Geling, A., Steiner, H., Willem, M., Bally-Cuif, L. and Haass, C. (2002) A gamma-secretase inhibitor blocks Notch signaling in vivo and causes a severe neurogenic phenotype in zebrafish. *EMBO Rep.*, **3**, 688–694.

57. Micchelli, C.A., Esler, W.P., Kimberly, W.T., Jack, C., Berezovska, O., Kornilova, A., Hyman, B.T., Perrimon, N. and Wolfe, M.S. (2003) Gamma-secretase/presenilin inhibitors for Alzheimer's disease phenocopy Notch mutations in Drosophila. *FASEB J.*, **17**, 79–81.

58. Wong, G.T., Manfra, D., Poulet, F.M., Zhang, Q., Josien, H., Bara, T., Engstrom, L., Pinzon-Ortiz, M., Fine, J.S., Lee, H.J. *et al.* (2004) Chronic treatment with the gamma-secretase inhibitor LY-411, 575 inhibits beta-amyloid peptide production and alters lymphopoiesis and intestinal cell differentiation. *J. Biol. Chem.*, **279**, 12876–12882.

59. Bateman, R.J., Siemers, E.R., Mawuenyega, K.G., Wen, G., Browning, K.R., Sigurdson, W.C., Yarasheski, K.E., Friedrich, S.W., Demattos, R.B., May, P.C. *et al.* (2009) A gamma-secretase inhibitor decreases amyloid-beta production in the central nervous system. *Ann. Neurol.*, **66**, 48–54.

60. Comery, T.A., Martone, R.L., Aschmies, S., Atchison, K.P., Diamantidis, G., Gong, X., Zhou, H., Kreft, A.F., Pangalos, M.N., Sonnenberg-Reines, J. *et al.* (2005) Acute gamma-secretase inhibition improves contextual fear conditioning in the Tg2576 mouse model of Alzheimer's disease. *J. Neurosci.*, **25**, 8898–8902.

61. D'Onofrio, G., Panza, F., Frisardi, V., Solfrizzi, V., Imbimbo, B.P., Paroni, G., Cascavilla, L., Seripa, D. and Pilotto, A. Advances in the identification of gamma-secretase inhibitors for the treatment of Alzheimer's disease. *Expert Opin. Drug Discov.*, **7**, 19–37.

62. Caspersen, C., Wang, N., Yao, J., Sosunov, A., Chen, X., Lustbader, J.W., Xu, H.W., Stern, D., McKhann, G. and Yan, S.D. (2005) Mitochondrial Abeta: a potential focal point for neuronal metabolic dysfunction in Alzheimer's disease. *FASEB J.*, **19**, 2040–2041.

63. Du, H., Guo, L., Fang, F., Chen, D., Sosunov, A.A., McKhann, G.M., Yan, Y., Wang, C., Zhang, H., Molkentin, J.D. *et al.* (2008) Cyclophilin D deficiency attenuates mitochondrial and neuronal perturbation and ameliorates learning and memory in Alzheimer's disease. *Nat. Med.*, **14**, 1097–1105.

64. Fang, D., Wang, Y., Zhang, Z., Du, H., Yan, S., Sun, Q., Zhong, C., Wu, L., Vangavaragu, J.R., Yan, S. *et al.* (2015) Increased neuronal PreP activity reduces Abeta accumulation, attenuates neuroinflammation and improves mitochondrial and synaptic function in Alzheimer disease's mouse model. *Hum. Mol. Genet.*, **24**, 5198–5210.

65. Fang, D., Zhang, Z., Li, H., Yu, Q., Douglas, J.T., Bratasz, A., Kuppusamy, P., Yan, S.S. (2016) Increased electron paramagnetic resonance signal correlates with mitochondrial dysfunction and oxidative stress in an Alzheimer's disease mouse brain. *J. Alzheimer's Dis.: JAD*, **51**, 571–580.

66. Livak, K.J. and Schmittgen, T.D. (2001) Analysis of relative gene expression data using real-time quantitative PCR and the 2(-Delta Delta C(T)) method. *Methods (San Diego, CA)*, **25**, 402–408.

67. Du, H., Guo, L., Yan, S., Sosunov, A.A., McKhann, G.M. and Yan, S.S. (2010) Early deficits in synaptic mitochondria in an Alzheimer's disease mouse model. *Proc. Natl. Acad. Sci. U. S. A.*, **107**, 18670–18675.

68. Du, H., Guo, L., Zhang, W., Rydzewska, M. and Yan, S. (2011) Cyclophilin D deficiency improves mitochondrial function and learning/memory in aging Alzheimer disease mouse model. *Neurobiol. Aging*, **32**, 398–406.

69. Du, F., Yu, Q., Yan, S., Hu, G., Lue, L.F., Walker, D.G., Wu, L., Yan, S.F., Tieu, K. and Yan, S.S. (2017) PINK1 signalling rescues amyloid pathology and mitochondrial dysfunction in Alzheimer's disease. *Brain*, **140**, 3233–3251.